

# Characteristic $L$ X-Ray Spectra from Proton, $\alpha$ -Particle, and Oxygen Bombardment of $\text{Sn}^\dagger$

David K. Olsen, C. Fred Moore, and Patrick Richard

Center for Nuclear Studies, University of Texas, Austin, Texas 78712

(Received 15 June 1972; revised manuscript received 4 January 1973)

Spectra have been measured [using a crystal (LiF;200) spectrometer] of  $L$  x rays produced by 2.0-MeV proton, 3.2-MeV  $\alpha$ -particle, and 30.0-MeV oxygen bombardment of thick tin targets.  $L$  x-ray lines are observed in the  $\alpha$ -particle-produced spectrum from initial configurations with up to four additional  $M$ -shell electron vacancies. The energy resolution of 8 eV (full width at half-maximum) did not allow any detailed structure to be resolved in the oxygen bombardment; an almost continuous structure is observed from multiply ionized tin. The ratios of x-ray yields from  $L+M$  vacancies to yields from  $L$  vacancies are shown to have the correct order of magnitude for a simultaneous direct Coulomb ionization process for proton and  $\alpha$ -particle impact.

## I. INTRODUCTION

Several experiments have been reported in which  $K$  x-ray lines<sup>1</sup> and  $L$  x-ray lines<sup>2</sup> produced by heavy-ion bombardment have been observed to be broadened and shifted to higher energies than the corresponding lines produced by proton and electron bombardment. For heavy-ion beams in the 1-MeV/amu range, these energy shifts have been attributed to multiple inner-shell electron vacancies of the initial atomic configurations produced by the atom-heavy-ion collisions. Recently high-resolution experiments using crystal spectrometers have resolved the shifted  $K\alpha$  and  $K\beta$  lines into parent and satellite components.<sup>3</sup> These satellite lines result from initial atomic configurations in which the heavy-ion collisions have removed from one to six  $2p$  electrons. Little high-resolution work has been done for heavy-ion-produced  $L$  x-ray transitions.<sup>4,5</sup>

Herein we report the measurement of  $L$  x-ray spectra produced from 2.0-MeV proton, 3.2-MeV  $\alpha$ -particle, and 30.0-MeV oxygen bombardment of thick tin targets. Using a crystal (LiF; 200) spectrometer, an energy resolution of 8 eV (full width at half-maximum) is obtained. All of the  $LN$  x-ray lines produced by the  $\alpha$ -particle bombardment are clearly observed to have satellite transitions resulting from  $M$ -shell electron vacancies. In particular, the intense  $L\beta_{2,15}$  transition is observed with zero to four electron vacancies in the  $M$  shell. A nearly continuous spectrum was observed from the oxygen bombardment where no detailed satellite structure could be resolved.

It is expected that if atom-atom collision effects<sup>6,7</sup> are not present, multiple inner-shell ionization can be explained by direct simultaneous Coulomb ionization of the atom by the incident projectile. Indeed, much work involving  $K\alpha$  x-ray satellite transitions has been reported which supports this assumption.<sup>8-10</sup> Der *et al.*<sup>5</sup> have shown that

the  $L$  x-ray energy shifts of highly ionized Ni, Cu, and Zn produced by oxygen bombardment decrease with increasing oxygen energy as do the  $M$ -shell Coulomb-ionization cross sections of the same energies. In this paper we show that the ratios of proton- and  $\alpha$ -particle-produced x-ray yields from  $L+M$  initial vacancies to yields from  $L$ -only initial vacancies have the correct order of magnitude for a simultaneous direct Coulomb reaction mechanism.

## II. EXPERIMENT

Beams of 30.0-MeV oxygen ions, 2.0-MeV protons and 3.2-MeV  $\alpha$  particles from The University of Texas at Austin EN tandem and KN Van de Graaff accelerators were focused into thick tin targets at an incidence angle of  $45^\circ$ . The resulting x rays were wavelength-analyzed by a Bragg crystal spectrometer positioned at  $90^\circ$  to the beam direction. The diffracted x rays from a LiF (200) crystal were detected in a flow-proportional counter operating at 2000 V using a 10% argon and 90% methane gas mixture. The spectrometer shared a common vacuum system with the beam line.

For each setting of the spectrometer, x rays were counted for a fixed amount of beam current. The number of x rays counted was then recorded and the angle of the spectrometer was changed by a stepping motor, so that the x-ray wavelength was incremented by a constant amount of 0.00123 Å. The data-accumulation system was automatic and was controlled by a PDP-7 computer. Each 1024-channel spectrum consists of many short data accumulations added together in order to reduce possible systematic errors. For the  $^1\text{H}^+$ ,  $^4\text{He}^+$ , and  $^{16}\text{O}^{5+}$ -produced spectra a total of approximately 25, 250, and 8  $\mu\text{C}$  of charge, respectively, was collected for each spectral datum.

## III. RESULTS AND DISCUSSION OF ENERGIES

The spectra produced by the proton,  $\alpha$ -particle, and oxygen bombardments are shown in Fig. 1,

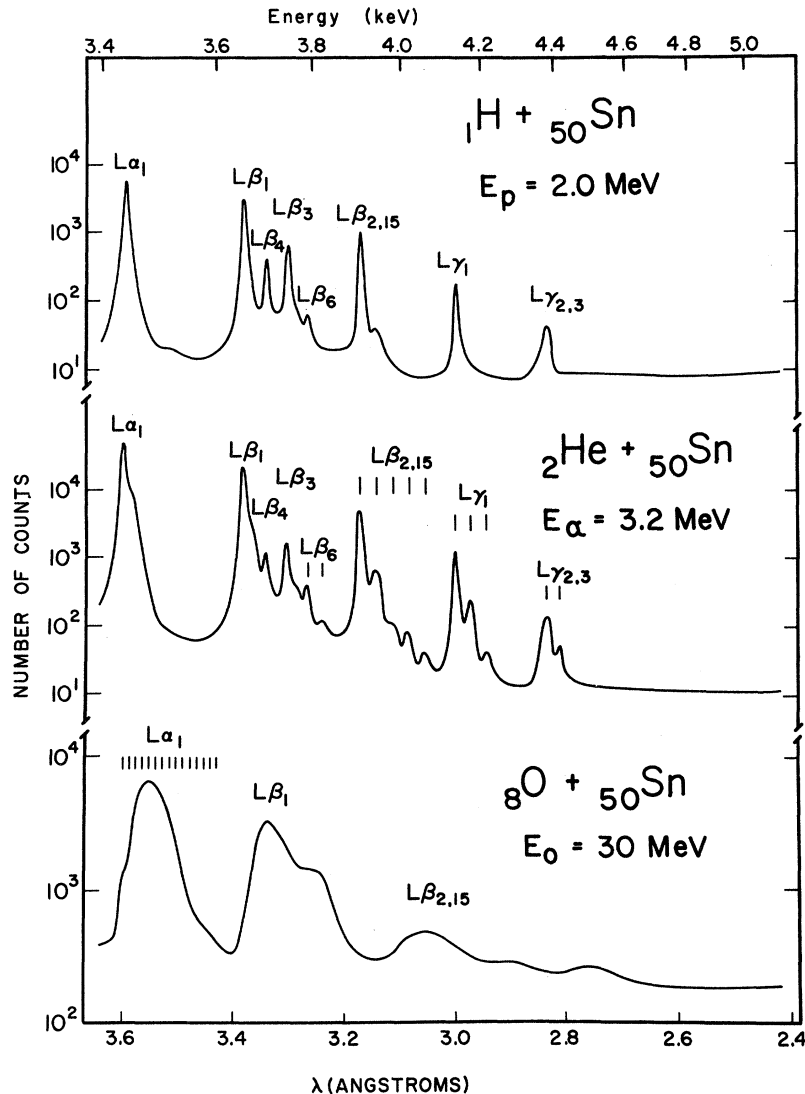


FIG. 1. Spectra of  $L$  x-ray lines from hydrogen, helium, and oxygen bombardment of tin. The short vertical lines below some peak labels indicate HFS-calculated energy shifts of these peaks for successively removing  $M$ -shell electrons from the atomic configurations. The spectra shown are smooth curves through discrete data. Each spectrum contained 1024 points. The error associated with each point is due to counting statistics and can thus be estimated from the scale.

where the number of counts per channel is plotted against the channel number which is proportional to the x-ray wavelength. At the top of the figure is shown an energy scale in units of keV. No self-absorption corrections have been applied to the spectra. Eight previously known  $L$  x-ray transitions are observed on the proton-produced spectrum.<sup>11</sup> The  $L\alpha_1$ ,  $L\beta_1$ ,  $L\beta_4$ , and  $L\beta_3$  lines are  $LM$  transitions, whereas the  $L\beta_6$ ,  $L\beta_{2,15}$ ,  $L\gamma_1$ , and  $L\gamma_{2,3}$  are  $LN$  transitions. In addition to these eight lines, eight new lines are observed on the  $\alpha$ -particle-produced spectrum. They have energies of  $3828 \pm 3$ ,  $3943 \pm 2$ ,  $3982 \pm 3$ ,  $4016 \pm 3$ ,  $4057 \pm 2$ ,  $4170 \pm 2$ ,  $4210 \pm 3$ , and  $4409 \pm 3$  eV. The 3943-eV line is also observed on the proton-produced spectrum.

These new lines occur at energies in multiples of from 32 to 41 eV higher in energy than the known

$LN$  transition energies, and must be due to additional electron vacancies produced in the ion-atom collisions. In order to determine the nature of this inner-shell multiple ionization, Hartree-Fock-Slater (HFS) calculations<sup>12</sup> were performed for the eight known  $L$  x-ray transitions observed on the proton-produced spectrum. Energy shifts were calculated for these transitions for initial atomic configurations with one additional electron vacancy in the  $2p$ ,  $3p$ ,  $3d$ ,  $4p$ , and  $4d$  shells, respectively. The results are listed in Table I. The  $2s$ ,  $3s$ , and  $4s$  shells were not considered, since large Coster-Kronig transition rates would transfer  $s$  vacancies to  $p$  vacancies of the same major shell. The energy shift of removing  $n$  electrons from a specific shell is approximately  $n$  times the energy shift for removing one electron from that shell.

TABLE I. Energy shifts in eV for Sn  $L$  x rays with additional electron holes.

x ray	Transition	Shell of additional electron hole				
		2p	3p	3d	4p	4d
$L\alpha_1$	$2p_{3/2} \rightarrow 3d_{5/2}$	85.4	11.2	11.5	0.6	0.5
$L\beta_1$	$2p_{1/2} \rightarrow 3d_{3/2}$	88.6	11.3	11.3	0.7	0.5
$L\beta_4$	$2s_{1/2} \rightarrow 3p_{1/2}$	74.2	10.7	13.7	0.5	0.5
$L\beta_8$	$2s_{1/2} \rightarrow 3p_{3/2}$	75.9	11.3	14.5	0.5	0.5
$L\beta_6$	$2p_{3/2} \rightarrow 4s_{1/2}$	119.5	31.9	34.9	3.1	1.9
$L\beta_{2,15}$	$2p_{3/2} \rightarrow 4d_{3/2}, 4d_{5/2}$	122.7	34.7	37.3	4.6	3.1
$L\gamma_1$	$2p_{1/2} \rightarrow 4d_{3/2}$	126.6	35.0	37.3	4.6	3.1
$L\gamma_{2,3}$	$2s_{1/2} \rightarrow 4p_{1/2}, 4p_{3/2}$	107.0	31.5	35.5	3.0	2.1

It is obvious from Table I that the energies of the newly observed transitions are consistent with additional  $M$ -shell electron vacancies. The 3943-, 3982-, 4016-, and 4057-eV lines are satellites of the intense  $L\beta_{2,15}$  transition with 1, 2, 3, and 4  $M$ -shell electron vacancies, respectively. The 4170- and 4210-eV lines are  $L\gamma_1$  transitions with one and two additional  $M$ -shell holes; and the 3828- and 4409-eV lines are satellites of the weak  $L\beta_6$  and  $L\gamma_{2,3}$  transition with one  $M$ -shell electron vacancy. In Fig. 1 the peak positions of these transitions are shown by the short vertical lines below the parent peak identification on the  $\alpha$ -particle-produced spectrum. No clearly resolved satellites of  $LM$  transitions are observed, since additional  $M$ -shell holes give energy shifts of about 13 eV. The energy resolution would not allow these weak satellites to be resolved, and the multiple electron vacancies manifest themselves as high-energy tails on these peaks. Such an effect is observed for the  $L\alpha_1$  line. Also, no transitions due to additional  $L$ -shell holes are observed from the

$\alpha$ -particle bombardment. Such a line for the  $L\alpha_1$  transition would occur at 3536 eV.

The energies of the newly observed transitions from the  $\alpha$ -particle spectrum are compared in detail with HFS calculations in Table II. Columns one and two list the transitions and their initial electron configurations. Column three gives the experimental energies of the parent transitions and their satellites. HFS-calculated energies are listed in columns four and five for both  $3p$  and  $3d$  holes. Since the electron vacancies can be from either or both shells, column six gives the average energy for  $3p$  and  $3d$  electron vacancies. The last four columns give the energy increase from the parent states for columns three to six. Whereas the HFS calculations reproduce the experimental transition energies to about 1%, the calculated energy shifts should be accurate to within 1 eV. In all cases the experimental energy shifts are in good agreement with the average HFS-calculated values. In addition, the widths of these satellite lines increase with increasing electron vacancies, further indicating that both  $3p$  and  $3d$  holes are responsible for them.

The oxygen-produced spectrum shown in Fig. 1 is completely different from the  $\alpha$ -particle and proton-produced spectra. With our energy resolution of 8 eV, an almost continuous spectrum of overlapping peaks from closely spaced satellite transitions is observed. The only discernible structures are a few very broad peaks shifted upwards in energy many tens of eV from the parent transitions. In particular, the centroid of the  $L\alpha_1$  line has shifted upwards 50 eV in the oxygen bombardment and has a width of 55 eV. This increase in centroid energy corresponds to an average initial configuration  $M$ -shell vacancy of four or five electrons. Clearly, the oxygen-produced spectrum re-

TABLE II. Observed and calculated energies of  $LN$  x-ray transitions in Sn.

x ray	Electron holes of initial state	Energies (eV)				Energy shifts (eV)			
		Observed	3p holes	3d holes	Average	Observed	3p holes	3d holes	Average
$L\beta_6$	$L$	3793	3783	3783	3783	...	...	...	...
	$L M$	$3828 \pm 3$	3815	3518	3816	$35 \pm 3$	32	35	33
$L\beta_{2,15}$	$L$	3905	3892	3892	3892	...	...	...	...
	$L M$	$3943 \pm 2$	3927	3929	3928	$38 \pm 2$	35	37	36
	$L M^2$	$3982 \pm 3$	3962	3969	3966	$77 \pm 3$	70	77	74
	$L M^3$	$4016 \pm 3$	3997	4008	4003	$111 \pm 3$	105	116	111
	$L M^4$	$4057 \pm 3$	4034	4049	4041	$152 \pm 3$	142	157	149
$L\gamma_1$	$L$	4131	4111	4111	4111	...	...	...	...
	$L M$	$4170 \pm 2$	4146	4148	4147	$39 \pm 2$	35	37	36
	$L M^2$	$4210 \pm 3$	4181	4188	4185	$79 \pm 3$	70	77	74
$L\gamma_{2,3}$	$L$	4377	4315	4315	4315	...	...	...	...
	$L M$	$4409 \pm 3$	4347	4351	4349	$32 \pm 3$	32	36	34

sults from many satellite transitions of initial configurations with many electron vacancies. The short vertical lines below the  $L\alpha_1$  peak identification for the oxygen-produced spectrum in Fig. 1 show peak positions for this transition for successively removing *M*-shell electrons.

#### IV. RESULTS AND DISCUSSION OF YIELD RATIOS

Having clearly established the nature of the x-ray satellite transitions produced by proton and  $\alpha$ -particle impact, we consider the reaction mechanism for producing this simultaneous *L*- and *M*-shell multiple ionization. Fano and Lichten<sup>6</sup> and Barat and Lichten<sup>7</sup> have proposed that multiple inner-shell ionization can occur through level crossings of the target and incident projectile. This electron-promotion mechanism is not expected to occur unless the binding energy of the electron to be promoted is less than the binding energies of the levels of the incident projectile.<sup>7</sup> Because the *M* shell of tin ( $\sim 600$  eV) is far more tightly bound than the *K* shell of hydrogen (13.6 eV) and helium (25.4 eV), the conditions for level crossings are not satisfied.

Many workers<sup>8-10</sup> have investigated a model for multiple Coulomb ionization which, by assuming the target electrons to be completely independent of each other, is just a simple extension of the classical<sup>13,14</sup> and semiclassical<sup>15</sup> formulations of single Coulomb ionization. We will show that the yield ratios of the *M*-shell satellite transitions observed in Fig. 1 are roughly consistent with the predictions of this reaction mechanism.

First we note for the specific cases considered here that the thick-target ratio of the x-ray yield with an initial state with one *L* vacancy and one *M* vacancy to the x-ray yield from one *L* vacancy only,  $Y_{LM}/Y_L$ , is approximately equal to the cross-section ratio  $\sigma_{LM}/\sigma_L$  for producing these ionizations. For 2.0-MeV protons and 3.2-MeV  $\alpha$  particles, the total tin *L* x-ray yield is increasing very rapidly with projectile energy.<sup>13-16</sup> In this case, as can be seen from Eq. (5.2) of Ref. 16,  $Y_{LM}/Y_L \approx \sigma_{LM}/\sigma_L$ , where effects due to the difference in fluorescence between the two ionization states are expected to be small<sup>17</sup> and are ignored. Although the x-ray yields are only partially resolved, we can estimate  $\sigma_{LM}/\sigma_L$  from the peak heights in Fig. 1. From the  $L\beta_{2,15}$  transitions on the proton-produced spectrum, we obtain  $\sigma_{LM}/\sigma_L \approx 0.05$  and, taking the average ratio from  $L\beta_8$ ,  $L\beta_{2,15}$ ,  $L\gamma_1$ , and  $L\gamma_{2,3}$  transitions on the  $\alpha$ -particle-produced spectrum, we obtain  $\sigma_{LM}/\sigma_L \approx 0.20$ . These ratios are believed to be accurate within a factor of 3, where most of the uncertainty is caused by the  $L_3$  and  $L_2$  absorption edges at 3928 and 4157 eV, respectively.

Formulations for multiple inner-shell ionization assuming independent electrons give<sup>9</sup>

$$\frac{\sigma_{LM}}{\sigma_L} \approx \frac{18P_M(E)}{1 - P_M(E)}, \quad (1)$$

where  $P_M(E)$  is the ionization probability per *M*-shell electron which has been assumed to be constant over the range of impact parameters for which the *L*-shell probability is not zero. The value of  $P_M(E)$  can be crudely estimated by the relation<sup>8</sup>

$$P_M(E) \approx \frac{\sigma_M(E)}{2\pi \langle r_M^2 \rangle}, \quad (2)$$

where  $\sigma_M(E)$  is the average ionization cross section per *M* electron and  $\langle r_M^2 \rangle$  is the average mean-square radius of the *M* shell.

We calculate  $\langle r_M^2 \rangle$  to be  $346 \times 10^{-20}$  cm<sup>2</sup> from the Herman-Skillman program.<sup>12</sup> The *M*-shell ionization cross sections were estimated using the classical binary-encounter model of Garcia.<sup>13</sup> This model predicts within a factor of 2 the experimental *M*-shell cross section for proton impact on Ho and Gd in the region of its maximum.<sup>13</sup> Both the 2.0-MeV protons and 3.2-MeV  $\alpha$  particles are in the region of maximum *M*-shell cross section and, using a weighted average binding energy of 612 eV, we obtain  $\sigma_M = 11 \times 10^{-20}$  cm<sup>2</sup> for protons and  $\sigma_M = 43 \times 10^{-20}$  cm<sup>2</sup> for  $\alpha$  particles. Using Eqs. (1) and (2), one obtains  $\sigma_{LM}/\sigma_L \approx 0.09$  for protons and  $\sigma_{LM}/\sigma_L \approx 0.36$  for  $\alpha$  particles. Considering the crudeness of our assumptions these order-of-magnitude estimates agree fortuitously well with the experimental cross-section ratios of 0.05 and 0.20, respectively.

#### V. CONCLUSIONS

These experimental results clearly establish enhanced simultaneous *L*- and *M*-shell multiple ionization by swift heavy charged-particle bombardment in the  $Z = 50$  region of the periodic table. With our energy resolution of 8 eV, only the *LN* x-ray satellite transitions due to additional *M*-shell vacancies produced by proton and  $\alpha$ -particle impact could be partially resolved. Significantly better resolution would be required to investigate satellites of *LN* transitions and the x-ray structure observed from oxygen bombardment.

Although the cross-section ratios for producing *L* and *M* vacancies to *L* vacancies only cannot be extracted accurately from the spectra, these ratios have the correct order of magnitude for a direct simultaneous Coulomb reaction mechanism. Only accurate measurements of these ratios as a function of bombarding energy or impact parameter would establish the validity of this mechanism for producing the multiple ionization reported here.

#### ACKNOWLEDGMENTS

The authors wish to thank Dr. H. Wolter for modifying and making a working version of the Herman-Skillman computer code available to us.

<sup>†</sup>Work supported in part by the Robert A. Welch Foundation and in part by the U. S. Atomic Energy Commission.

<sup>1</sup>P. Richard, I. L. Morgan, T. Furuta, and D. Burch, *Phys. Rev. Lett.* **23**, 1009 (1969); D. Burch and P. Richard, *Phys. Rev. Lett.* **25**, 983 (1970).

<sup>2</sup>P. H. Mokler, *Phys. Rev. Lett.* **26**, 811 (1970); S. Datz, C. D. Moak, B. R. Appleton, and T. A. Carlson, *Phys. Rev. Lett.* **27**, 363 (1971); D. Burch and P. Richard, *Bull. Am. Phys. Soc.* **16**, 74 (1971); H. Kamada, T. Tamura, and M. Teresawa (unpublished).

<sup>3</sup>A. R. Knudson, D. J. Nagel, P. G. Burkhalter, and K. L. Dunning, *Phys. Rev. Lett.* **26**, 1149 (1971); D. Burch, P. Richard, and R. L. Blake, *Phys. Rev. Lett.* **26**, 100 (1971); D. G. McCrary and P. Richard, *Phys. Rev. A* **5**, 1249 (1972).

<sup>4</sup>P. G. Burkhalter, A. R. Knudson, and D. J. Nagel, *Bull. Am. Phys. Soc.* **17**, 500 (1972).

<sup>5</sup>R. C. Der, R. J. Fortner, T. M. Kavanagh, J. M. Khan, and J. D. Garcia, *Phys. Lett.* **36A**, 239 (1971).

<sup>6</sup>U. Fano and W. Lichten, *Phys. Rev. Lett.* **14**, 627 (1965).

<sup>7</sup>M. Barat and W. Lichten, *Phys. Rev. A* **6**, 211 (1972).

<sup>8</sup>D. Burch, in International Conference on Inner-Shell Ionization, Atlanta, Ga., 1972 (unpublished).

<sup>9</sup>J. M. Hansteen and O. P. Mosebekk, *Phys. Rev. Lett.* **29**, 1361 (1972).

<sup>10</sup>A. R. Knudson, P. G. Burkhalter, and D. J. Nagel, in International Conference on Inner-Shell Ionization, Atlanta, Ga., 1972 (unpublished); S. Hansen, J. H. McGuire, and R. L. Watson (to be published); M. J. Saltmarsh, A. van der Woude, and C. A. Ludemann, *Phys. Rev. Lett.* **29**, 392 (1972); J. H. McGuire and M. H. Mittleman, *Phys. Rev. A* **5**, 1971 (1972); R. L. Kauffman, C. F. Moore, P. Richard, and J. H. McGuire, C. F. Moore, D. K. Olsen, and R. L. Kauffman (unpublished).

<sup>11</sup>J. A. Bearden, *Rev. Mod. Phys.* **31**, 1 (1967).

<sup>12</sup>F. Herman and S. Skillman, *Atomic Structure Calculations* (Prentice-Hall, Englewood Cliffs, N. J., 1963).

<sup>13</sup>J. D. Garcia, *Phys. Rev. A* **1**, 280 (1970).

<sup>14</sup>M. Gryzinski, *Phys. Rev.* **138**, A336 (1965).

<sup>15</sup>J. Bang and J. M. Hansteen, *K. Dan. Vidensk. Selsk. Mat.-Fys. Medd.* **31**, No. 13 (1959).

<sup>16</sup>E. Merzbacher and H. W. Lewis, in *Encyclopedia of Physics*, edited by S. Flügge (Springer-Verlag, Berlin, 1958), Vol. 34, p. 166.

<sup>17</sup>F. P. Larkins, *J. Phys. B* **4**, L29 (1971).

## Electrocaloric Effect in Fluids and Its Relationship with Nonlinear Light Scattering\*

K. H. Wang<sup>†</sup> and R. M. Herman

The Pennsylvania State University, University Park, Pennsylvania 16802

(Received 20 November 1972)

We derive an equation describing the electrocaloric effect in fluids, which differs from that predominantly employed in current theoretical studies of nonlinear optics. The consequent alterations in the predictions of nonlinear optical theory and in the interpretation of experimental observations are then described.

### I. INTRODUCTION

In recent years, stimulated light scattering from isobaric temperature (entropy) excitations in liquids has acquired importance by itself, as well as in conjunction with other scattering mechanisms.<sup>1-3</sup> The first reported observation of stimulated thermal scattering (STS) was that of Rank, Cho, Foltz, and Wiggins<sup>4</sup> following the theoretical description by Herman and Gray<sup>5</sup> who indicated the importance of the absorptive heating mechanism in light scattering. (We call this phenomenon STS-II, in conformity with current practice.) Almost simultaneously, Zaitzev, Kyzylasov, Starunov, and Fabelinski<sup>6</sup> reported the discovery of a scattering phenomenon in benzene and methanol which they attributed to the generation of entropy waves through the electrocaloric effect (STS-I). Following this, Mash *et al.*<sup>7</sup> observed a scattering in gaseous H<sub>2</sub> which they also attributed to the electrocaloric coupling.

In the literature which has followed, however, there has not been complete agreement on the form

for the electrocaloric coupling leading to STS-I. Most investigators<sup>1,3,6-9</sup> appear to have used equations describing the energy balance in fluids of the form

$$\rho C_v \frac{\partial T}{\partial t} - \frac{(\gamma - 1)C_v}{\beta} \frac{\partial \rho}{\partial t} = \dot{Q} + \lambda \nabla^2 T, \quad (1)$$

with

$$\dot{Q} = -\frac{1}{8\pi} T_0 \left( \frac{\partial \epsilon}{\partial T} \right)_p \frac{\partial E^2}{\partial t}, \quad (2)$$

while others<sup>10,11</sup> have employed Eq. (1) with  $\dot{Q}$  given, instead, by

$$\dot{Q} = -\frac{1}{8\pi} T_0 \left( \frac{\partial \epsilon}{\partial T} \right)_p \frac{\partial E^2}{\partial t}. \quad (3)$$

In still another treatment,<sup>2</sup> Eq. (3) is taken to be valid and then, without elaboration, the authors allow that it is acceptable to employ Eq. (2) when describing STS-I.

The notation in these equations is standard,  $\rho$  and  $T$  being density and pressure variations from the corresponding equilibrium values  $\rho_0$  and  $T_0$ ,